

PVP2006-ICPVT-11-93645

CALANDRIA TUBE TO TUBESHEET ROLLER-EXPANDED JOINT QUALIFICATION

A.S. Banwatt, R.G. Sauvé

Atomic Energy of Canada Limited
2251 Speakman Drive
Mississauga, Ontario, Canada, L5K 1B2

ABSTRACT

The complex calandria tube to calandria tubesheet roller-expanded joint in CANDU nuclear reactors is usually qualified by test. In this paper, a state-of-the-art numerical simulation is undertaken in order to improve the understanding of the behaviour of the joint to support design modifications and provide assurance that the test rig envelopes behaviour of the in-situ reactor assembly. Parameters such as hoop stress, and plastic deformation of the assembly are predicted. The analysis results are also compared with the available test data and in-situ experimental data. The analysis results show that the test performed to qualify the joint using a small plate and single joint is representative of the in-situ reactor configuration.

INTRODUCTION

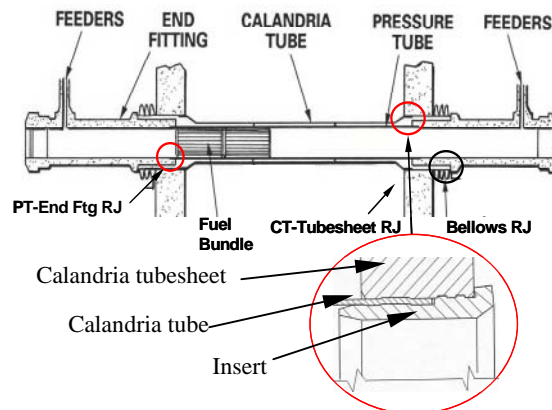
In CANDU nuclear power reactors, the interface between the calandria tube to calandria tubesheet (Figure 1) is a roller-expanded joint between two dissimilar materials. The calandria tube is sandwiched between the calandria tubesheet and the sleeve insert, the latter having an external land that matches with the grooves in the tubesheet. During the roller expanding operation, the land of the sleeve deforms the calandria tube into the tubesheet groove and the grooves in the outer side of the tubesheet bore are penetrated by the outer surface of the sleeve, thereby providing the required strength and leak tightness.

As part of the joint qualification process, the joint is roller-expanded using a test rig to represent the in reactor configuration. The test rig is fabricated using a 12 inch x 12 inch x 1.25 inch thick plate with actual geometries for the roller expanded area. Dimensional measurements are taken at the insert surface and the joint surfaces are etched to study the material grain flow patterns. The objective of this paper is to describe the process used to qualify the complex fabrication of a key reactor component using predictive methodology in conjunction with limited testing.

The predictive models, representing the test rig and the actual roller expanded joint in the reactor are developed and carried out using the H3DMAP [1] computer program, which is a nonlinear, three-dimensional continuum mechanics finite element analysis program used to solve a wide variety of finite deformation problems. In this application, a modified explicit algorithm is employed that accounts for the non-inertial transient nature that is present in certain classes of manufacturing applications (i.e. deformation-induced residual stresses

and manufacturing processes) and directly provides for elastic spring back thus providing accurate estimates of residual stress. Among the salient features of this application are the three dimensional, large deformation contact and material constitutive models. The numerical algorithms employed in this assessment have been shown to provide excellent results through experimental validations [3,4] conducted on various roller expansion configurations.

Figure 1: Calandria Tube to Calandria Tubesheet Roller-Expanded Joint



The results obtained from the test rig are compared with those from the computer analysis runs. In addition, a comparison is also made with the in-situ sleeve insert data obtained from the reactor site. Following computer code validation with the test rig results, the methodology is applied to the in situ reactor configuration. A 25-lattice pitch model is developed with one central location modeled in detail. Comparison is made for the flow patterns, effective plastic strains and stresses between the two analysis models.

A quantitative assessment is made based on the element hoop stresses, which are directly related to the radial stress and considered to be important for the pressure retaining capability of the joint. Based on the hoop stress and strains it is demonstrated that the test rig model results envelopes the actual in situ reactor model. The rolled joint expansion analysis was further extended to predict the joint pull out loads. These results were compared with the experimental data, where failure occurred in the calandria tube away from the rolled joint.

The results are shown to be consistent with experimental results and demonstrate that the roller-expanded joint is stronger than the calandria tube away from the rolled joint area for the pull-out conditions.

DESCRIPTION

Three dimensional finite element model topology for the test rig and the actual in-situ rolled joint configuration in the reactor are developed using the FEMAP pre- and post-processor [2]. The models are run using the nonlinear finite element computer code H3DMAP to simulate the rolling process and determine the plastic strains and residual stresses. The results of the test rig and reactor models are compared to establish the validity of the test rig in representing the in-situ reactor configuration. The rolled joint geometric dimensions are the same in both the models. Differences are in the tubesheet dimensions, where the tubesheet/baffle plate configuration is represented by an equivalent 1.25" thick plate.

Materials used for the calandria tube and the calandria tubesheet are Zircaloy-2 and 304L stainless steel respectively. The calandria tubesheet sleeve insert material is 304L fully annealed stainless steel. The available information at room temperature was used for the analysis. The detailed stress-strain curves derived from the available data are shown in Figure 2, and represent the average of the actual values obtained from various material test reports and available literature. Isotropic material properties are considered in this assessment. For these materials, representative engineering stress-strain data are converted to true stress-strain data, which is input in the finite element model. The material properties for the rollers do not have a significant effect on the analyses as the input motion is prescribed at the roller nodes. For display purposes the roller material is considered to be elastic.

ACCEPTANCE CRITERIA

The stresses in the roller-expanded area are generated by the elasto-plastic deformation field. The damage criterion (i.e., acceptance criterion) is based on the maximum effective plastic strain reached at rupture. This is an average rupture strain, which is estimated based on the experimental stress-strain data. Allowable effective plastic strains over a cross-section considered for the stainless steel and Zircaloy-2 are 0.46 and 0.3 respectively. These strains provide the limit for incipient plastic instability (i.e. necking).

ASSUMPTIONS

The simulations undertaken in this work are subject to the following assumptions:

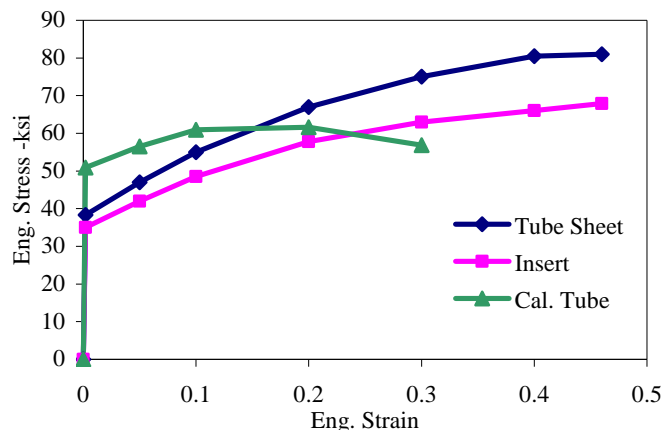
- Only a small part of the calandria tube in the reactor is modelled as it is considered that the remainder of the tube has an insignificant effect on the rolling behaviour of the joint. No boundary conditions are applied to the calandria tube.
- The test rig is considered fixed in three translational directions at the middle of the four corner edges of the plate (i.e., no clearance is considered between the bolts and the hole).
- The material properties used in the analyses are based on test and/or experimental data.
- The roller expansion process is simulated by applying an equivalent specified roller radial velocity to obtain the required radial displacement. The roller assembly is subject to the rotational spin of the assembly during roller expansion as explained in the section under Input Motion.

METHODOLOGY

The roller expansion simulation is performed using the H3DMAP Version 7 computer code [1]. The code employs the nonlinear explicit analysis option for solid mechanics, which is based on finite element formulations [5] suitable for finite deformation problems.

Analysis is performed using the non-inertial transient analysis option, where the hybrid explicit/dynamic relaxation solution option [6] is invoked. In this solution procedure, the mass is scaled such that the critical time step for each element is equal to the final time specified in the forcing function definition divided by the number of cycles required. This procedure is well suited to manufacturing problems, as the converged residual stress fields are determined in a single unloading step without the need for special treatment.

Figure 2: Engineering Stress-Engineering Strain for Tubesheet, Insert and Calandria Tube



FINITE ELEMENT MODELS

For the simulation, a test rig model and a 25-hole model representing the in-reactor calandria tube/calandria tubesheet roller-expanded joints are developed. The test rig model has eight small holes around the circumference, which are designed for subsequent axial pull tests. The reactor model is developed using a configuration representing 25 lattice sites. One site location at the centre is modelled in detail, while the other sites are approximated by an equivalent diameter based on an average of the calandria tubesheet and calandria insert diameters. The centre site, which is modelled in detail, is similar in both the models. The test rig model with eight-small holes around the circumference (Figure 3) is built using nonlinear hexahedron solid elements. The element formulation is iso-parametric under-integrated with unified hourglass control [5]. The test rig model contains 96,979 nodes and 83,752 hexahedron elements. The full reactor model is made up of 146,051 nodes and 118,688 hexahedron elements, Figure 4. The element aspect ratios are carefully controlled in the area of interest. A vertical section of the rolled joint through the centre hole is shown in Figure 5. The five-roller tool is modeled using surface (shell) elements. A section of the roller in contact with the insert is shown in Figure 5. To provide the proper interface between the various joint surfaces, contact surfaces, using a symmetric contact algorithm option, are used. The contact interfaces considered in the analysis are given in Table 1. The friction model considered both the Coulomb and Shear model.

Table 1: Contact Interface Friction Coefficients

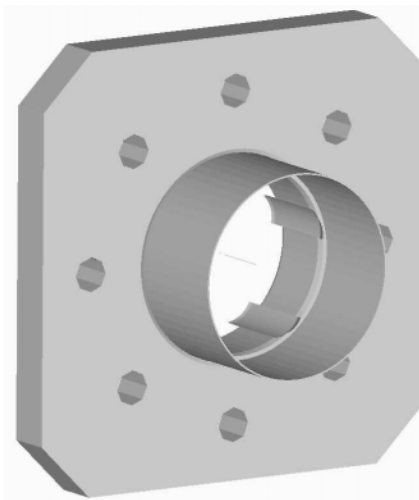
Joint	Friction Coefficient
Calandria Tubesheet – Sleeve Insert	0.3
Calandria Tubesheet – Calandria Tube	0.3
Calandria Tube and Sleeve Insert	0.3
Roller and Sleeve Insert	0.0

BOUNDARY CONDITIONS

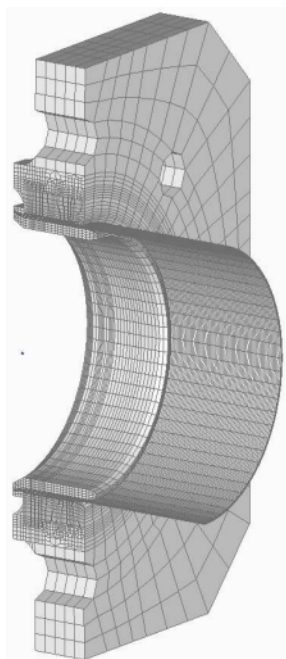
In the case of the test rig model, the nodes in the middle of the four corner edges of the model are fixed in the three translational degrees of freedom. For the 25-hole reactor tubesheet model, the outer edges are

fixed in all the translational degrees of freedom. For the roller-expanded area of interest, these boundary conditions are expected to represent the in situ reactor configuration. Roller nodes are fixed in the axial translational degree of freedom. Input motion is applied at the roller nodes in the radial direction. The spin of the roller surfaces is specified as constant and twelve revolutions of the roller assembly are considered.

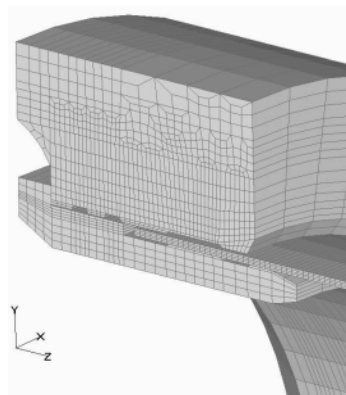
Figure 3: Test Rig Finite Element Model



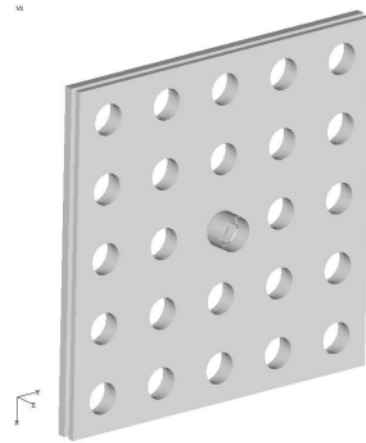
Test Rig Model



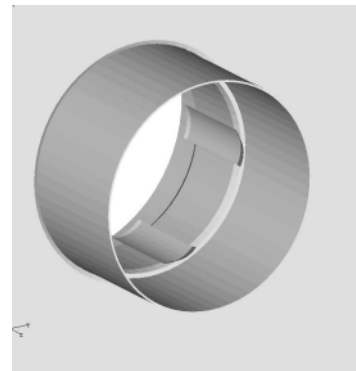
Section Through Centre Hole



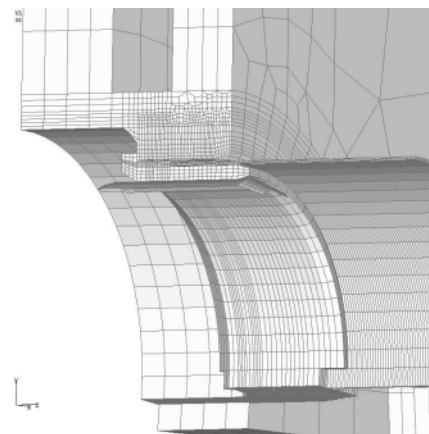
Exploded Section



Reactor Model



View Through Centre Hole



Exploded Section

Figure 4: Calandria Tubesheet/Calandria Tube Finite Element Reactor Model

Figure 5: Detailed Section through Vertical Axis - Central Hole

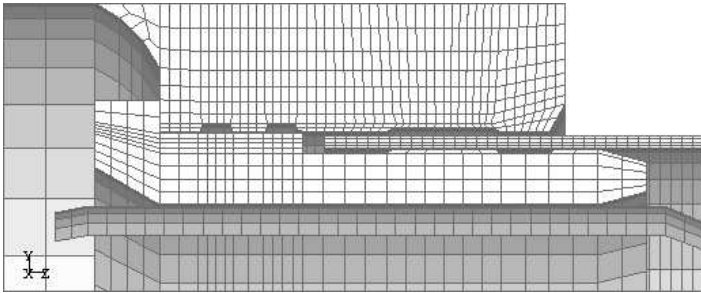
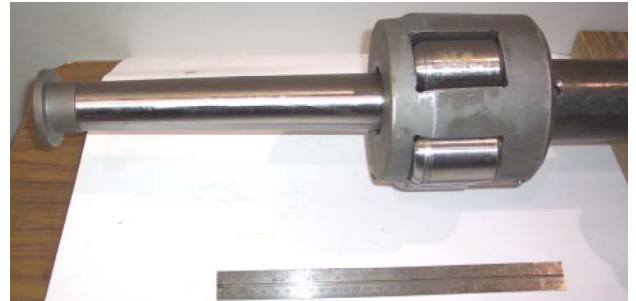
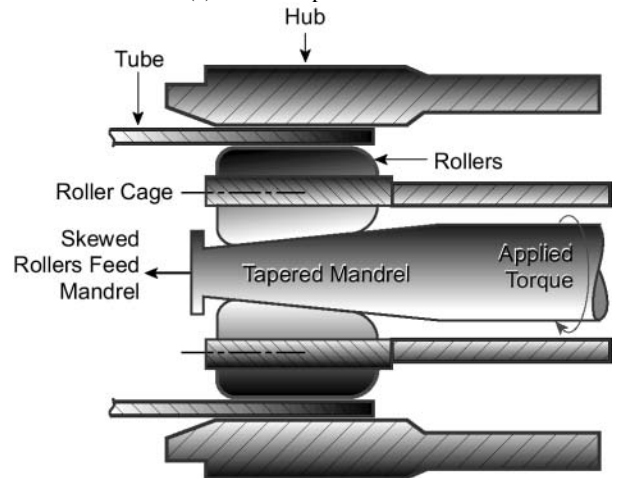


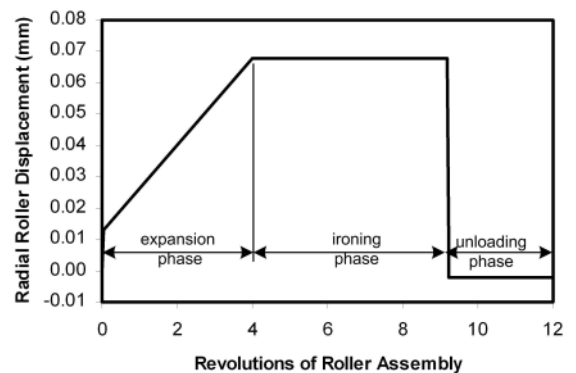
Figure 6: Roller Expansion Tool and Input Motion (a) Roller Expansion Tool, (b) Schematic of the Generic Roller Expansion Assembly, and (c) Roller Input Motion



(a) Roller Expansion Tool



(b) Schematic of the Generic Roller Expansion Assembly



(c) Programmed Roller Expansion of Input Motion

INPUT MOTION

Figures 6 (a) and (b) show the roller expansion tool and the Schematic of the Generic Roller Expansion Assembly. The tapered mandrel is moved forward, which in turn expands the rollers outwards. Once the roller assembly starts expanding, the clearances between the components are taken up. This is followed by the extrusion phase once plasticity is initiated by the radial expansion of the rollers. The final phase of roller radial expansion is the ironing phase (roller rotation at constant radial displacement) at the end of the extrusion. Once the rollers are retracted, the joint is left in a state of residual stress due to constraints provided by the tubesheet material around the joint. Input motion of the roller is adjusted to give the correct amount of radial expansion required at the tubesheet/calandria tube location and is shown in the Figure 6 (c).

RESULTS

Two finite element models representing the test rig and reactor calandria tube/tubesheet models are run using the H3DMAP computer program. The quantitative assessment is based on element results.

Figures 7 and 8 show the results for the hoop stresses and effective plastic strains. In these figures the scales reflect the actual minimum/maximum values corresponding to each run so that a proper comparison of the minimum/maximum values can be made of the differences in the rolled joint area in both of the analysis models.

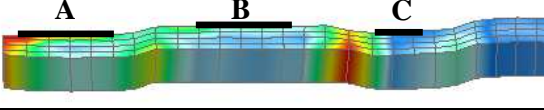
Radial stresses in the test rig configurations are generally similar, except for some local areas, particularly at the thin section of the calandria tube and at the tubesheet/insert mid section. There is significant variation due to the localized nature of the stresses at the discontinuities, i.e. at the slot corners. The major component of stress, the hoop stress S_{22} (Figure 7), provides the basis for comparison in both cases. Effective plastic strain, (Figure 8), is another parameter that provides a good comparison. Overall plastic deformation in all the cases is quite similar except for some local areas. Calandria tube stresses are considered in more detail. Figure 8 shows that the reactor model has generally slightly higher effective plastic strains. Similarly, a comparison is made of the nodal plastic strains for the various calandria tube areas. It indicates that, in the reactor model, critical areas B and C (Figure in Table 2) generally result in slightly higher effective plastic strains.

Radial compressive stresses at the calandria tube interface ensure leak tightness of the joint. Due to these compressive stresses, the calandria tube thickness is reduced during extrusion.

A comparison of the element average stresses is made at the selected areas A, B and C marked with solid lines (see figure included with Table 2), and the results are given in Table 2. Effective plastic strains at areas B and C are higher in the full reactor model. At the critical location, where the calandria tube is pinched between the tubesheet and the insert (between area B and C, Table 2), the test rig and reactor models average strains are 0.1211 and 0.1236 respectively.

Table 2: Calandria Tube Plastic Strains

Area*	A	B	C
Elements	27021 to 27041	27049 to 27076	27089 to 27100
Full Model	0.096	0.084	0.0837
Test Rig - 8 holes	0.1321	0.079	0.0785



*Areas are marked with dark black lines

Stresses are calculated for a sectioned quarter model in the circumferential direction for 16 elements. Figure 9 shows the comparison of effective plastic strains for the insert, calandria tube and tubesheet. The strains are generally similar in both the cases. Hoop stresses are plotted for the same components in Figure 10, which indicate that the hoop stresses are generally higher in the reactor case for the components of interest (i.e. calandria tube and calandria tubesheet). From this it can be inferred that the test rig model envelops and provides a reasonable representation of the reactor model. Symbols used in these figures are:

- TS-ID – Tube Sheet Internal Diameter
- S22 – Hoop Stress
- CT – Calandria Tube
- 8 – Test Rig Model
- F – Reactor Model

To quantify the differences between the two cases, element hoop stresses are averaged in the rolled joint region, where element numbers in that region range from 27017 to 27100.

Average hoop stresses for the reactor and test rig models are 35,454 psi and 32,270 psi. These results show that the hoop stress in the test rig is lower by 8.9% compared to in the reactor model case.

Radial contact stresses calculated for the reactor and test rig models are 625 psi and 570 psi respectively.

These results show that the reactor model and test rig model results are comparable, which demonstrates that the test rig model provides a reasonable representation of the reactor configuration.

To demonstrate the convergence of the results, the final converged maximum residual hoop stress and maximum effective plastic strain distributions in the test rig model are given in Figure 11, where maximum values are observed at the local discontinuities. Note the near axisymmetric distribution of the contours.

VERIFICATION

The input data are verified against the site rolling data. Information available from the site Process Record Sheets is the initial insert inside diameter before rolling and after rolling. The difference in the insert inside diameter before and after rolling is in the range of 0.087 inch and 0.099 inch, thus giving an average value of 0.048 inch. The corresponding expansion of insert radius used in the analysis is 0.054 inch, which is considered to be in reasonable agreement with the test data.

Figure 7: Rolled Joint Hoop Stresses (a) Reactor Model and (b) Test Rig

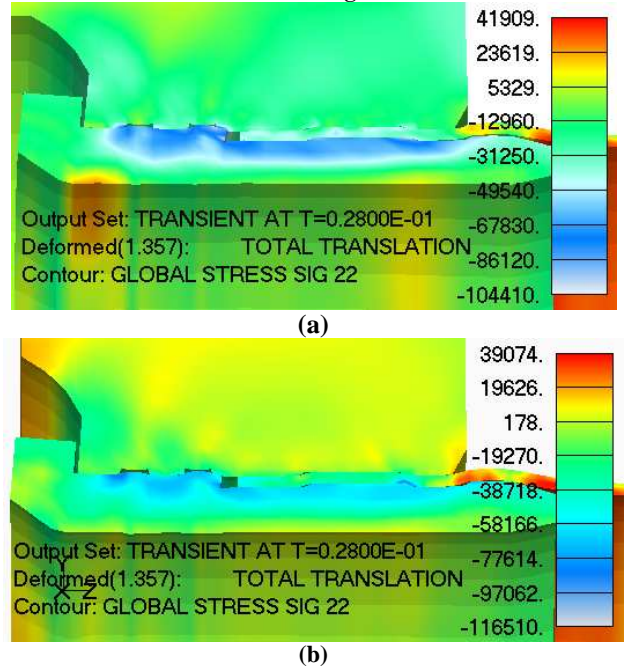


Figure 8: Rolled Joint Effective Plastic Strains (a) Reactor Model and (b) Test Rig

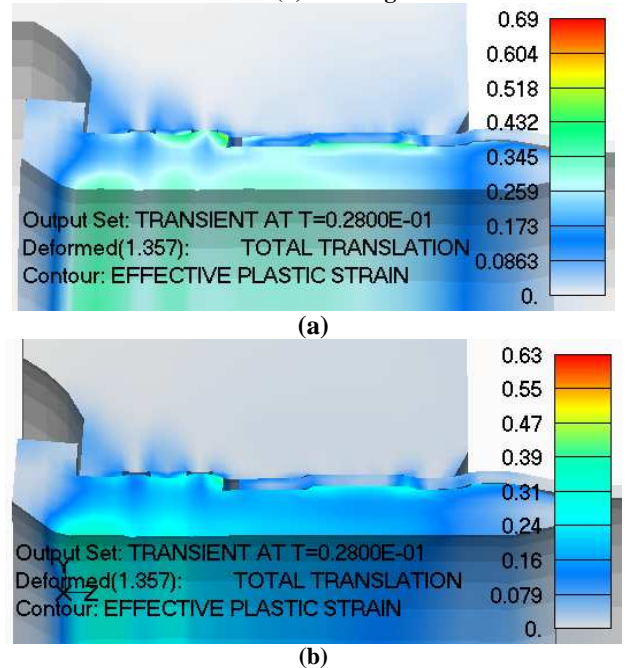
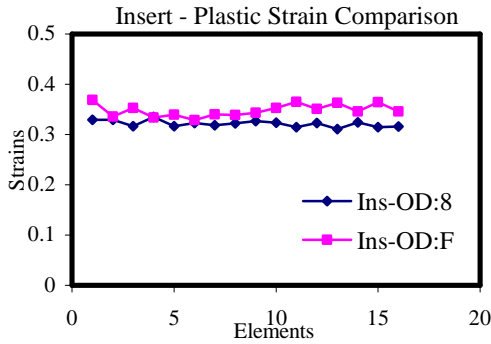
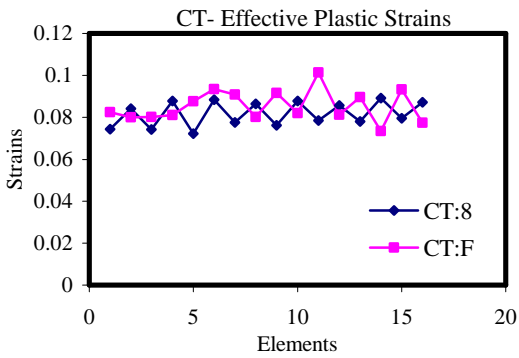


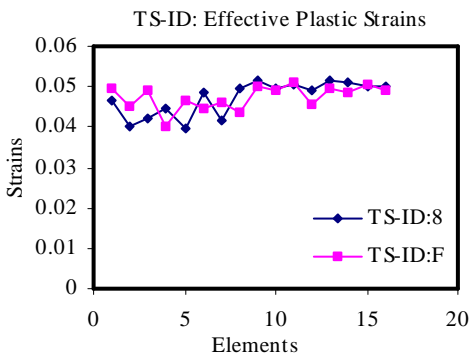
Figure 9: Comparison of Plastic Strains Between Sectioned Reactor Model and Test Rig (a) Insert, (b) Calandria Tube and (c) Tubesheet



(a)

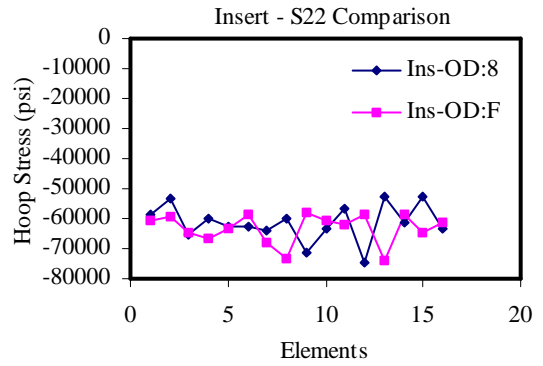


(b)

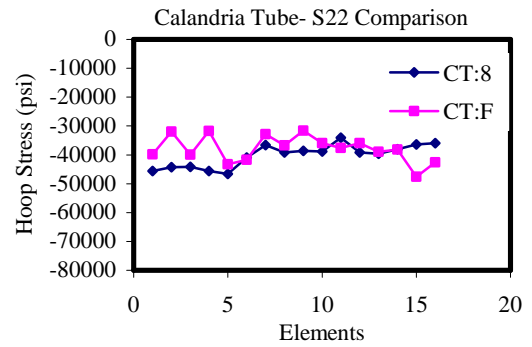


(c)

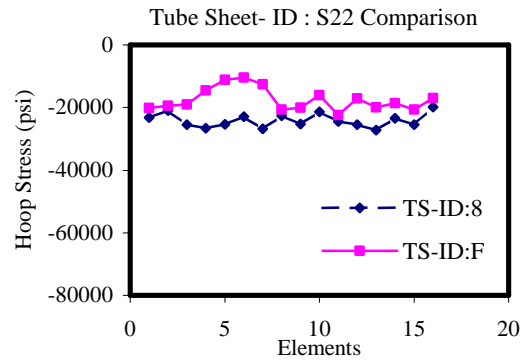
Figure 10: Comparison of Hoop Stresses between Sectioned Reactor Model and Test Rig (a) Insert, (b) Calandria Tube and (c) Tubesheet



(a)



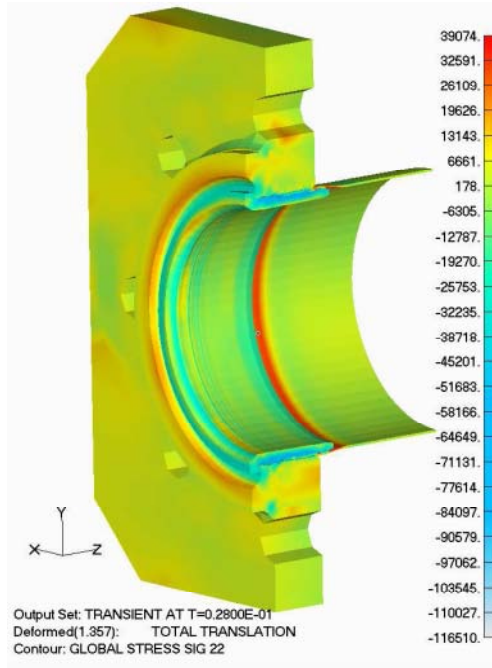
(b)



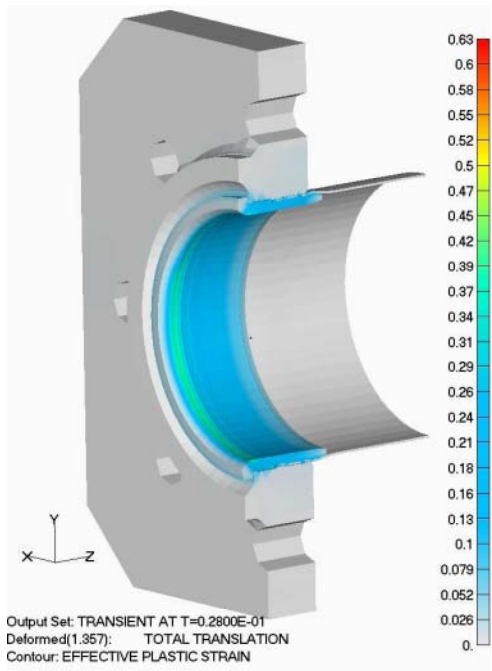
(c)

The calandria tube/calandria tubesheet rolled joint final deformed shape produced in a test rig is shown in Figure 12. Comparing the deformed pattern with the predicted pattern from Figures 7 and 8, it is observed that the deformation is markedly similar.

Figure 11: Overall Residual Hoop Stress and Effective Plastic Strain Distributions in Test Rig Model



Hoop Stress



Effective Plastic Strain

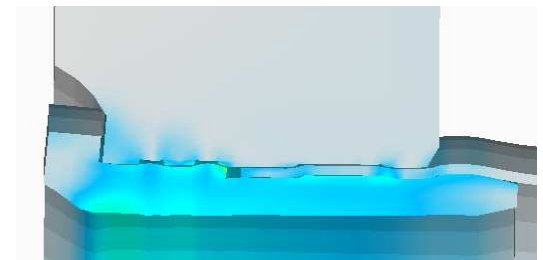
ASSESSMENT OF JOINT PULL OUT STRENGTH

The pull out strength of the roller-expanded joint is also investigated. Load is applied incrementally at the middle of the four corner edges of the test rig model to study the joint behaviour. The total maximum resultant load in the axial direction is 70,000 lbf. The calandria tube end nodes are fixed in the three translational directions.

Figure 12: Experimental Results of Roller Expanded Joint



Experiment – Test Rig



Prediction -Analysis

Calculations were restarted from the previous roller expansion analysis and continued with the following changes:

- The roller elements are made inactive.
- The hybrid explicit dynamic relaxation option is changed to a normal explicit nonlinear option, which is considered to be consistent with the pullout load application.
- The load history transient time is extended from the previous roller expansion run time.
- A concentrated nodal force of 70,000 lbf is incrementally applied at the middle of the four corner tubesheet edges, which had previously been fixed (i.e., the constraints in the axial direction are removed).
- Nodes on the free end of the calandria tube are fixed in all the translational directions.

In the following section, results of calandria tube pullout loads obtained from the finite element analysis are compared with those from the test rig experimental data. The pullout strength of the roller-expanded joint was not readily available from the test rig. Configuration of the test rig resulted in failure of the calandria tube remote from the joint. Thus, it was expected that the pullout load leading to the failure of the calandria tube in the test rig is lower than the joint pullout load. For this reason, the analysis model focused on the joint pullout load. This indicates consistency with the results obtained in the test rig.

EXPERIMENTAL AND ANALYSIS RESULTS

For the Test Rig pull out strength, a small portion of the calandria tube (23.5 inch, considered to be adequate) is used in the rolled joint. From inspection of the failed specimen, it appears that the failure occurred in the calandria tube due to large strains following necking. Therefore, it is concluded that the rolled joint is considered to be stronger than the calandria tube. The material starts yielding at a load of 35,000 lbf (start of necking) and fails at a load of 55,000 lbf.

The analysis results should be considered preliminary, as no tuning of the results was done. The material properties used are those at room temperature and no credit is taken for the anisotropic properties of the material. Failure occurred in the rolled joint near the red area in Figure 13 (denoted here as the pinched area). At this section the material thickness is reduced by 0.010 inch, i.e., the remaining material thickness at the section is $0.049 - 0.010 = 0.039$ inch (about 20% reduction in thickness). In the analysis model, only the flared end of the tube is modelled with 0.049 inch thickness, a 4 inch length and 8.06 inch outside diameter. Therefore the results obtained from the analysis are for the rolled joint strength. The results are:

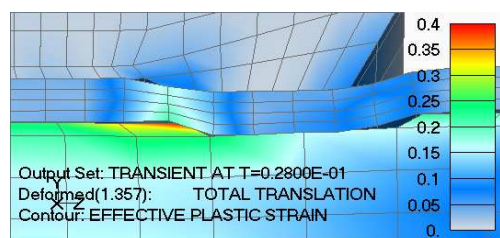
- Start of necking at the pinched area = 42,000 lbf (yielding through the calandria tube thickness).
- Material rupture at pinched area = 62,000 lbf (instability at large strain).

Roller joint failure occurs at the pinched area (Figure 13). If required the roller joint pull out strength can be increased by slightly varying the slot dimensions.

Experimental data is only available for the case of calandria tube failure. However, the joint pullout strength is expected to be somewhat higher for the following reasons.

- The calandria tube diameter is slightly bigger at the roller joint area.
- The calandria tube material has work hardened in that area and the analysis assumes that the material is at room temperature.
- The experiment was carried out at a higher temperature and the material in the predictive model was taken to be at room temperature.

Figure 13: Calandria Tube Pinched Area Between the Calandria Tubesheet and Insert



A review of the deformed calandria tube configuration highly magnified, Figure 13, indicates that the results can be improved by refining the mesh in the calandria tube pinched area.

Also the joint strength can be further increased by simply adjusting the dimensions of the insert and slightly reducing the deformation in the pinched area. However, the results based on the current configuration are considered to be reasonable.

CONCLUSIONS

A test rig model and a reactor calandria tube/tubesheet roller expanded joint model have been developed and analyzed. The results are compared with the available site data. The following conclusions are drawn for these results:

The test rig model is considered to produce similar plastic strains in both the test and reactor models. The average hoop stress was approximately 9% lower in the case of the test rig. This provides assurance that the results obtained using the test rig are both representative and conservative in comparison to the reactor case from the stand point of leak tightness.

In the pull out test, failure occurred in the calandria tube remote from the joint, which was the focus in the finite element calculations. The joint pullout strength is expected to be marginally higher as the material has work hardened in that area. Given that the differences can be rationalized and no tuning of input parameters was undertaken, it is, nevertheless, clear that the finite element model is in good accord with the currently available experimental data.

REFERENCES

1. Sauv , R.G., Morandin, G., "Computer Program Documentation User Manual Programmer Manual - H3DMAP Version 7, A Three Dimensional Finite Element Computer Code for Linear and Nonlinear Continuum Mechanics", AECL Report No. CW-114515-225-001 R0, 2004 May.
2. FEMAP 8.2 Manual Finite Element Modelling and Post-processing, Structural Dynamics Research Corporation, 2003.
3. Metzger, D.R., Sauv , R.G., Nadeau, E., "Prediction of Residual Stresses by Simulation of the Rolled Joint Manufacturing Process for Steam Generators", ASME PVP, v 305, Current Topics in Computational Mechanics, 1995, p 67-74.
4. Metzger, D.R., Sauv , R.G., "Computation of Residual Stress Distribution in Tubes Due to a Rolled Joint Forming Process", ASME PVP, v 235, Design and Analysis of Pressure Vessels, Piping, and Components - 1992, 1992, p 209-214.
5. Metzger, D., Sauv , R.G., "Three Dimensional Hourglass Stabilization for One Point Quadrature Finite Elements", in Design Analysis, Robust Methods, and Stress Classification, ASME PVP, v 265, 1993.
6. Sauv , R.G., Metzger, D.R., "A Hybrid Explicit Solution Technique for Quasi-Static Transients", ASME PVP, v 326, Computer Technology - 1996: Applications and Methodology, 1996, p 151-157.